

RESEARCH

Open Access

Low-rank filter and detector for multidimensional data based on an alternative unfolding HOSVD: application to polarimetric STAP

Maxime Boizard^{1,2*}, Guillaume Ginolhac³, Frédéric Pascal² and Philippe Forster¹

Abstract

This paper proposes an extension of the higher order singular value decomposition (HOSVD), namely the alternative unfolding HOSVD (AU-HOSVD), in order to exploit the correlated information in multidimensional data. We show that the properties of the AU-HOSVD are proven to be the same as those for HOSVD: the orthogonality and the low-rank (LR) decomposition. We next derive LR filters and LR detectors based on AU-HOSVD for multidimensional data composed of one LR structure contribution. Finally, we apply our new LR filters and LR detectors in polarimetric space-time adaptive processing (STAP). In STAP, it is well known that the response of the background is correlated in time and space and has a LR structure in space-time. Therefore, our approach based on AU-HOSVD seems to be appropriate when a dimension (like polarimetry in this paper) is added. Simulations based on signal-to-interference-plus-noise ratio (SINR) losses, probability of detection (Pd), and probability of false alarm (Pfa) show the interest of our approach: LR filters and LR detectors which can be obtained only from AU-HOSVD outperform the vectorial approach and those obtained from a single HOSVD.

Keywords: Multilinear algebra; HOSVD; Low-rank approximation; STAP; Low-rank filter; Low-rank detector

1 Introduction

In signal processing, more and more applications deal with multidimensional data, whereas most of the signal processing algorithms are derived based on one- or two-dimensional models. Consequently, multidimensional data have to be folded as vector or matrix to be processed. These operations are not lossless since they involve a loss of structure. Several issues may arise from this loss: decrease of performances and lack of robustness (see for instance [1]). The multilinear algebra [2,3] provides a good framework to exploit these data by preserving the structure information. In this context, data are represented as multidimensional arrays called tensor. However, generalizing matrix-based algorithms to the multilinear algebra framework is not a trivial task. In particular, some multilinear tools do not retain all the properties of the vectorial and matrix tools. Let us consider the case of the

singular value decomposition (SVD). The SVD decomposes a matrix into a sum of rank-1 matrices and has uniqueness and orthonormality properties. There is no single multilinear extension of the SVD, with exactly the same properties as the SVD. Depending on which properties are preserved, several extensions of the SVD have been introduced.

On one hand, CANDECOMP/PARAFAC (CP) [4] decomposes a tensor as a sum of rank-1 tensors, preserving the definition of rank. Due to its properties of identifiability and uniqueness, this decomposition is relevant for multiple parameter estimation. CP was first introduced in the signal processing community for direction of arrival (DOA) estimation [5,6]. New decompositions were then derived from CP. For example, in [7,8], a decomposition based on a constrained CP model is applied to multiple-input multiple-output (MIMO) wireless communication system. These decompositions share a common issue for some applications: they are not orthogonal.

On the other hand, the higher order singular value decomposition (HOSVD) [3,9] decomposes a tensor as a product of a core tensor and a unitary matrix for each

*Correspondence: maxime.boizard@lss.supelec.fr

¹SATIE, ENS Cachan, 61, av President Wilson, Cachan 94230, France

²SONDRA, Supélec, 3 rue Joliot-Curie, Gif-sur-Yvette 91192, France

Full list of author information is available at the end of the article

dimension of the tensor. This decomposition relies on matrix unfoldings. In general, HOSVD does not have the properties of identifiability and uniqueness. The model provided by HOSVD is defined up to a rotation. It implies that HOSVD cannot be used for multiple parameters estimation unlike CP. Orthogonality properties of HOSVD allow to extend the low-rank methods such as [10,11]. These methods are based on the ranks of the different matrix unfoldings, called p -ranks [2,12,13]. HOSVD has been successfully applied in many fields such as image processing [14], sonar and seismo-acoustic [15], ESPRIT [16], ICA [17], and video compression [18].

HOSVD is based on the classic tensor unfolding and in particular on the matrix of left singular vectors. This unfolding transforms a tensor into a matrix in order to highlight one dimension. In other words, HOSVD only considers simple information, which is the information contained in each dimension taken separately. The correlated information, which is the information contained in a combination of dimensions, is neglected. In [19], a new decomposition, PARATREE^a, based on the sequential unfolding SVD (SUSVD) was proposed. This decomposition considers some correlated information, using the right matrix of the singular vectors. This approach can be improved, to consider any type of correlated information. Consequently, we propose to develop a new set of orthogonal decompositions which will be called alternative unfolding HOSVD (AU-HOSVD). In this paper, we will define this new operator and study its main properties, especially the extension of the low-rank approximation. We will show the link between AU-HOSVD and HOSVD.

Based on this new decomposition, we derive new low-rank (LR) filters and LR detectors for multidimensional data containing a target embedded in an interference. We assume that the interference is the sum of two noises: a white Gaussian noise and a low-rank structured one. In order to illustrate the interest of these new LR filters and LR detectors, we will consider the multidimensional space-time adaptive processing (STAP). STAP is a technique used in airborne phased array radar to detect moving target embedded in an interference background such as jamming (jammers are not considered in this paper) or strong ground clutter [20] plus a white Gaussian noise (resulting from the sensor noise). While conventional radars are capable of detecting targets both in the time domain related to target range and in the frequency domain related to target velocity, STAP uses an additional domain (space) related to the target angular localization. From the Brennan rule [21], STAP clutter is shown to have a low-rank structure^b. That means that the clutter response in STAP is correlated in time and space. Therefore, if we add a dimension, the LR filter and LR detector based on HOSVD will not be interesting. In this

paper, we show the interest of our new LR filters and LR detectors based on AU-HOSVD in a particular case of multidimensional STAP: polarimetric STAP [22]. In this polarimetric configuration, each element transmits and receives in both H and V polarizations, resulting in three polarimetric channels (HH, VV, HV/VH). The dimension of the data model is then three. Simulations based on signal-to-interference-plus-noise ratio (SINR) losses [20], probability of detection (Pd), and probability of false alarm (Pfa) show the interest of our approach: LR filters and LR detectors which are obtained using AU-HOSVD outperform the vectorial approach and those obtained from HOSVD in the general polarimetry model (the channels HH and VV are not completely correlated). We believe that these results could be extended to more generalized multidimensional STAP systems like MIMO-STAP [23-26].

The paper is organized as follows. Section 2 gives a brief overview of the basic multilinear algebra tools. In particular, the HOSVD and its main properties are presented. In Section 3, the AU-HOSVD and its properties are derived. Section 4 is devoted to the derivation of the LR filters and LR detectors based on AU-HOSVD. Finally, in Section 5, these new tools are applied to the case of polarimetric STAP.

The following convention is adopted: scalars are denoted as italic letters, vectors as lowercase boldface letters, matrices as boldface capitals, and tensors as boldface calligraphic letters. We use the superscripts ^H for Hermitian transposition and * for complex conjugation. The expectation is denoted by $E[\cdot]$, and the Frobenius norm is denoted $\|\cdot\|$.

2 Some basic multilinear algebra tools

This section contains the main multilinear algebra tools used in this paper. Let $\mathcal{H}, \mathcal{B} \in \mathbb{C}^{I_1 \times \dots \times I_P}$, be two P th-order tensors and $h_{i_1 \dots i_P}, b_{i_1 \dots i_P}$ their elements.

2.1 Basic operators of multilinear algebra

Unfoldings In this paper, three existing unfoldings are used; for a general definition of tensor unfolding, we refer the reader to [2].

- Vector: vec transforms a tensor \mathcal{H} into a vector, $vec(\mathcal{H}) \in \mathbb{C}^{I_1 I_2 \dots I_P}$. We denote vec^{-1} , the inverse operator.
- Matrix: this operator transforms the tensor \mathcal{H} into a matrix $[\mathcal{H}]_p \in \mathbb{C}^{I_p \times I_1 \dots I_{p-1} I_{p+1} \dots I_P}$, $p = 1 \dots P$. For example, $[\mathcal{H}]_1 \in \mathbb{C}^{I_1 \times I_2 \dots I_P}$. This transformation allows to enhance simple information (i.e., information contained in one dimension of the tensor).
- Square matrix: this operator transforms a $2P$ th-order tensor $\mathcal{R} \in \mathbb{C}^{I_1 \times I_2 \dots \times I_P \times I_1 \times I_2 \dots \times I_P}$ into a square

matrix, $SqMat(\mathcal{R}) \in \mathbb{C}^{I_1 \dots I_P \times I_1 \dots I_P}$. $SqMat^{-1}$ is the inverse operator.

The inverse operators always exist. However, the way the tensor was unfolded must be known.

Products

- The scalar product $\langle \mathcal{H}, \mathcal{B} \rangle$ of two tensors is defined as

$$\begin{aligned} \langle \mathcal{H}, \mathcal{B} \rangle &= \sum_{i_1} \sum_{i_2} \dots \sum_{i_P} b_{i_1 i_2 \dots i_P}^* h_{i_1 i_2 \dots i_P} \\ &= \text{vec}(\mathcal{B})^H \text{vec}(\mathcal{H}). \end{aligned} \quad (1)$$

It is the usual Hermitian scalar product in linear spaces [12,27].

- Let $\mathbf{E} \in \mathbb{C}^{I_n \times I_n}$ be a matrix, the n -mode product between \mathbf{E} and a tensor \mathcal{H} is defined as

$$\begin{aligned} \mathcal{G} &= \mathcal{H} \times_n \mathbf{E} \in \mathbb{C}^{I_1 \times \dots \times I_n \times \dots \times I_P} \\ \iff (\mathcal{G})_{i_1 \dots j_n \dots i_P} &= \sum_{i_n} h_{i_1 \dots i_n \dots i_P} e_{j_n i_n} \\ \iff [\mathcal{G}]_n &= \mathbf{E} [\mathcal{H}]_n. \end{aligned} \quad (2)$$

- The outer product between \mathcal{H} and \mathcal{B} , $\mathcal{E} = \mathcal{H} \circ \mathcal{B} \in \mathbb{C}^{I_1 \times \dots \times I_P \times I_1 \times \dots \times I_P}$ is defined as

$$e_{i_1 \dots i_P i_1 \dots i_P} = h_{i_1 \dots i_P} b_{i_1 \dots i_P}. \quad (3)$$

Tensor ranks There are two concepts of rank for tensors:

- The tensor rank: it is defined as the minimum number of rank-1 tensors (for example a P th-order rank-1 tensor can be written as the outer product of P vectors) necessary to obtain the considered tensor.
- The p -ranks: they are defined as the ranks of the unfoldings, $r_p = \text{rank}([\mathcal{H}]_p)$.

2.2 Higher order singular value decomposition

This subsection recalls the main results on the HOSVD used in this paper.

Theorem 2.1. *The higher order singular value decomposition (HOSVD) is a particular case of Tucker decomposition [9] with orthogonality properties. HOSVD decomposes a tensor \mathcal{H} as follows [3]:*

$$\mathcal{H} = \mathcal{K} \times_1 \mathbf{U}^{(1)} \dots \times_P \mathbf{U}^{(P)}, \quad (4)$$

where $\forall n, \mathbf{U}^{(n)} \in \mathbb{C}^{I_n \times I_n}$ is an orthonormal matrix and $\mathcal{K} \in \mathbb{C}^{I_1 \times \dots \times I_P}$ is the core tensor, which satisfies the all-orthogonality conditions [3]. The matrix $\mathbf{U}^{(n)}$ is given by the singular value decomposition of the n -dimension

unfolding, $[\mathcal{H}]_n = \mathbf{U}^{(n)} \Sigma^{(n)} \mathbf{V}^{(n)H}$. Using classical unfolding, the HOSVD only considers the simple information.

Remark Let $\mathcal{H} \in \mathbb{C}^{I_1 \times I_2 \times \dots \times I_P \times I_1 \times I_2 \times \dots \times I_P}$ be a $2P$ th-order Hermitian tensor, i.e., $h_{i_1, \dots, i_P, j_1, \dots, j_P} = h_{j_1, \dots, j_P, i_1, \dots, i_P}^*$. The HOSVD of \mathcal{H} is written as [16]

$$\mathcal{H} = \mathcal{K} \times_1 \mathbf{U}^{(1)} \dots \times_P \mathbf{U}^{(P)} \times_{P+1} \mathbf{U}^{(1)*} \dots \times_{2P} \mathbf{U}^{(P)*}. \quad (5)$$

The following result permits to compute a tensor approximation of lower p -ranks.

Proposition 2.1 (Low-rank approximation). *Let us introduce $\mathcal{H} = \mathcal{H}_c + \mathcal{H}_0$. \mathcal{H}_c is a (r_1, \dots, r_P) low-rank tensor where $r_k < I_k$, for $k = 1, \dots, P$. An approximation of \mathcal{H}_0 is given by [15,27]:*

$$\mathcal{H}_0 \approx \mathcal{H} \times_1 \mathbf{U}_0^{(1)H} \mathbf{U}_0^{(1)} \dots \times_P \mathbf{U}_0^{(P)H} \mathbf{U}_0^{(P)}, \quad (6)$$

with $\mathbf{U}_0^{(n)} = [\mathbf{u}_{r_n+1}^{(n)} \dots \mathbf{u}_{I_n}^{(n)}]$.

It is well known that this solution is not optimal in the sense of least squares. However, it is a correct approximation in most cases [16,27] and it is easy to implement. That is why iterative algorithms will not be used in this paper.

2.3 Covariance tensor and estimation

Definition Let $\mathcal{Z} \in \mathbb{C}^{I_1 \times \dots \times I_P}$ be a random P th-order tensor, and the covariance tensor $\mathcal{R} \in \mathbb{C}^{I_1 \times \dots \times I_P \times I_1 \times \dots \times I_P}$ is defined as [28]

$$\mathcal{R} = E[\mathcal{Z} \circ \mathcal{Z}^*]. \quad (7)$$

Sample covariance matrix Let $\mathbf{z} \in \mathbb{C}^{I_1 \times \dots \times I_P}$ be a zero-mean Gaussian random vector and $\mathbf{R} \in \mathbb{C}^{I_1 \times \dots \times I_P \times I_1 \times \dots \times I_P}$ its covariance matrix. Let \mathbf{z}_k be K observations of \mathbf{z} . The sample covariance matrix (SCM), $\hat{\mathbf{R}}$, is written as follows:

$$\hat{\mathbf{R}} = \frac{1}{K} \sum_{k=1}^K \mathbf{z}_k \mathbf{z}_k^H. \quad (8)$$

Sample covariance tensor Let $\mathcal{Z}_k \in \mathbb{C}^{I_1 \times \dots \times I_P}$ be K observations of \mathcal{Z} . By analogy with the SCM, $\hat{\mathcal{R}} \in \mathbb{C}^{I_1 \times \dots \times I_P \times I_1 \times \dots \times I_P}$, the sample covariance tensor (SCT) is defined as [16]

$$\hat{\mathcal{R}} = \frac{1}{K} \sum_{k=1}^K \mathcal{Z}_k \circ \mathcal{Z}_k^*. \quad (9)$$

Remark If we denote $\mathbf{z} = \text{vec}(\mathcal{Z})$, then

$$\mathbf{R} = SqMat(\mathcal{R}). \quad (10)$$

3 Alternative unfolding HOSVD

Due to proposition 2.1, it is possible to design LR filters based on HOSVD. This approach does not work when all p -ranks are full (i.e., $r_p = I_p$, $p = 1 \dots P$), since no projection could be done. However, the data may still have

a LR structure. This is the case of correlated data where one or more ranks relative to a group of dimensions are deficient. Tensor decompositions allowing to exploit this kind of structure have not been promoted. To fill this gap, we propose to introduce a new tool which will be able to extract this kind of information. This section contains the main contribution of this paper: the derivation of the AU-HOSVD and its principal properties.

3.1 Generalization of standard operators

Notation of indices In order to consider correlated information, we introduce a new notation for the indices of a tensor. We consider $\mathcal{H} \in \mathbb{C}^{I_1 \times \dots \times I_P}$, a P th-order tensor. We denote $\mathbb{A} = \{1, \dots, P\}$ the set of the dimensions and $\mathbb{A}_1, \dots, \mathbb{A}_L$, L subsets of \mathbb{A} which define a partition of \mathbb{A} . In other words, $\mathbb{A}_1, \dots, \mathbb{A}_L$ satisfy the following conditions:

- $\mathbb{A}_1 \cup \dots \cup \mathbb{A}_L = \mathbb{A}$
- They are pairwise disjoint, i.e., $\forall i \neq j, \mathbb{A}_i \cap \mathbb{A}_j = \emptyset$.

Moreover $\mathbb{C}^{I_1 \dots I_P}$ is denoted $\mathbb{C}^{I_{\mathbb{A}}}$. For example, when $\mathbb{A}_1 = \{1, 2\}$ and $\mathbb{A}_2 = \{3, 4\}$, $\mathbb{C}^{I_{\mathbb{A}_1} \times I_{\mathbb{A}_2}}$ means $\mathbb{C}^{I_1 I_2 \times I_3 I_4}$.

A generalization of unfolding in matrices In order to build our new decomposition, we need a generalized unfolding, adapted from [2]. This operator allows to unfold a tensor into a matrix whose dimensions could be any combination \mathbb{A}_l of the tensor dimensions. It is denoted as $[\cdot]_{\mathbb{A}_l}$, and it transforms \mathcal{H} into a matrix $[\mathcal{H}]_{\mathbb{A}_l} \in \mathbb{C}^{I_{\mathbb{A}_l} \times I_{\mathbb{A} \setminus \mathbb{A}_l}}$.

A new unfolding in tensors We denote as *Reshape* the operator which transforms a tensor \mathcal{H} into a tensor $\text{Reshape}(\mathcal{H}, \mathbb{A}_1, \dots, \mathbb{A}_L) \in \mathbb{C}^{I_{\mathbb{A}_1} \times \dots \times I_{\mathbb{A}_L}}$ and Reshape^{-1} the inverse operator.

A new tensor product The n -mode product allows to multiply a tensor with a matrix along one dimension. We propose to extend the n -mode product to multiply a tensor with a matrix along several dimensions, combined in \mathbb{A}_l . Let $\mathbf{D} \in \mathbb{C}^{I_{\mathbb{A}_l} \times I_{\mathbb{A}_l}}$ be a square matrix. This new product, called multimode product, is defined as

$$\mathcal{B} = \mathcal{H} \times_{\mathbb{A}_l} \mathbf{D} \iff [\mathcal{B}]_{\mathbb{A}_l} = \mathbf{D} [\mathcal{H}]_{\mathbb{A}_l}. \quad (11)$$

The following proposition shows the link between multimode product and n -mode product.

Proposition 3.1 (Link between n -mode product and multimode product). Let $\mathcal{H} \in \mathbb{C}^{I_1 \times \dots \times I_P}$ be a P th-order tensor, $\mathbb{A}_1, \dots, \mathbb{A}_L$ be a partition of \mathbb{A} , and $\mathbf{D} \in \mathbb{C}^{I_{\mathbb{A}_l} \times I_{\mathbb{A}_l}}$ be a square matrix. Then, the following equality is verified:

$$\begin{aligned} \text{Reshape}(\mathcal{H} \times_{\mathbb{A}_l} \mathbf{D}, \mathbb{A}_1, \dots, \mathbb{A}_L) \\ = \text{Reshape}(\mathcal{H}, \mathbb{A}_1, \dots, \mathbb{A}_L) \times_l \mathbf{D} \end{aligned} \quad (12)$$

Proof 3.1. The proof of Theorem 3.1 relies on the following straightforward result:

$$\forall l \in [1, L], [\mathcal{H}]_{\mathbb{A}_l} = [\text{Reshape}(\mathcal{H}, \mathbb{A}_1, \dots, \mathbb{A}_L)]_l.$$

This leads to $[\mathcal{B}]_{\mathbb{A}_l} = [\text{Reshape}(\mathcal{B}, \mathbb{A}_1, \dots, \mathbb{A}_L)]_l$ and $[\mathcal{H}]_{\mathbb{A}_l} = [\text{Reshape}(\mathcal{H}, \mathbb{A}_1, \dots, \mathbb{A}_L)]_l$. Applying these two results on (11), we obtain

$$\begin{aligned} [\text{Reshape}(\mathcal{B}, \mathbb{A}_1, \dots, \mathbb{A}_L)]_l \\ = \mathbf{D} [\text{Reshape}(\mathcal{H}, \mathbb{A}_1, \dots, \mathbb{A}_L)]_l. \end{aligned} \quad (13)$$

From Equation 2, Equation 13 is equivalent to

$$\text{Reshape}(\mathcal{B}, \mathbb{A}_1, \dots, \text{Reshape}(\mathcal{H}, \mathbb{A}_1, \dots, \mathbb{A}_L) \times_l \mathbb{A}_L) \mathbf{D}.$$

Finally, one has

$$\begin{aligned} \text{Reshape}(\mathcal{H} \times_{\mathbb{A}_l} \mathbf{D}, \mathbb{A}_1, \dots, \mathbb{A}_L) \\ = \text{Reshape}(\mathcal{H}, \mathbb{A}_1, \dots, \mathbb{A}_L) \times_l \mathbf{D}. \end{aligned}$$

Remark Thanks to the previous proposition and the commutative property of n -mode product, multimode product is also commutative.

3.2 AU-HOSVD

With the new tools presented in the previous subsection, we are now able to introduce the AU-HOSVD. This is the purpose of the following theorem.

Theorem 3.1 (Alternative unfolding HOSVD). Let $\mathcal{H} \in \mathbb{C}^{I_1 \times \dots \times I_P}$ and $\mathbb{A}_1 \dots \mathbb{A}_L$ a partition of \mathbb{A} . Then, \mathcal{H} may be decomposed as follows:

$$\mathcal{H} = \mathcal{K}_{\mathbb{A}_1/\dots/\mathbb{A}_L} \times_{\mathbb{A}_1} \mathbf{U}^{(\mathbb{A}_1)} \dots \times_{\mathbb{A}_L} \mathbf{U}^{(\mathbb{A}_L)}, \quad (14)$$

where

- $\forall l \in [1, L], \mathbf{U}^{(\mathbb{A}_l)} \in \mathbb{C}^{\mathbb{A}_l \times \mathbb{A}_l}$ is unitary. The matrix $\mathbf{U}^{(\mathbb{A}_l)}$ is given by the singular value decomposition of the \mathbb{A}_l -dimension unfolding, $[\mathcal{H}]_{\mathbb{A}_l} = \mathbf{U}^{(\mathbb{A}_l)} \Sigma^{(\mathbb{A}_l)} \mathbf{V}^{(\mathbb{A}_l)H}$.
- $\mathcal{K}_{\mathbb{A}_1/\dots/\mathbb{A}_L} \in \mathbb{C}^{I_1 \times \dots \times I_P}$ is the core tensor. It has the same properties as the HOSVD core tensor.

Notice that there are several ways to decompose a tensor with the AU-HOSVD. Each choice of the $\mathbb{A}_1, \dots, \mathbb{A}_L$ gives a different decomposition. For a P th-order tensor, the number of different AU-HOSVD is given by the Bell number, B_P :

$$\begin{aligned} B_1 &= 1 \\ B_{P+1} &= \sum_{k=1}^P \binom{P}{k} B_k. \end{aligned}$$

The AU-HOSVD associated to the partition $\mathbb{A}_1, \dots, \mathbb{A}_L$ is denoted $\text{AU-HOSVD}_{\mathbb{A}_1, \dots, \mathbb{A}_L}$.

Proof 3.2. First, let us consider $\mathbb{A}_1, \dots, \mathbb{A}_L$, a partition of \mathbb{A} . $\text{Reshape}(\mathcal{H}, \mathbb{A}_1 \dots \mathbb{A}_L)$ is a L th-order tensor and may be decomposed using the HOSVD:

$$\text{Reshape}(\mathcal{H}, \mathbb{A}_1, \dots, \mathbb{A}_L) = \mathcal{K} \times_1 \mathbf{U}^{(1)} \dots \times_L \mathbf{U}^{(L)}, \quad (15)$$

where the matrix $\mathbf{U}^{(l)}$ is given by the singular value decomposition of the l -dimension unfolding, $[\text{Reshape}(\mathcal{H}, \mathbb{A}_1, \dots, \mathbb{A}_L)]_l = [\mathcal{H}]_{\mathbb{A}_l} = \mathbf{U}^{(l)} \Sigma^{(l)} \mathbf{V}^{(l)H}$.

Since the matrices $\mathbf{U}^{(l)}$'s are unitary, Equation 15 is equivalent to

$$\text{Reshape}(\mathcal{H}, \mathbb{A}_1, \dots, \mathbb{A}_L) \times_1 \mathbf{U}^{(1)H} \dots \times_L \mathbf{U}^{(L)H} = \mathcal{K}. \quad (16)$$

Then, using proposition 3.1, the following equality is true:

$$\begin{aligned} &\text{Reshape}(\mathcal{H}, \mathbb{A}_1, \dots, \mathbb{A}_L) \times_1 \mathbf{U}^{(1)H} \dots \times_L \mathbf{U}^{(L)H} \\ &= \text{Reshape}(\mathcal{H} \times_{\mathbb{A}_1} \mathbf{U}^{(1)H} \dots \times_{\mathbb{A}_L} \mathbf{U}^{(L)H}, \\ &\quad \mathbb{A}_1, \dots, \mathbb{A}_L), \end{aligned} \quad (17)$$

which leads to

$$\text{Reshape}(\mathcal{H} \times_{\mathbb{A}_1} \mathbf{U}^{(1)H} \dots \times_{\mathbb{A}_L} \mathbf{U}^{(L)H}, \mathbb{A}_1, \dots, \mathbb{A}_L) = \mathcal{K}. \quad (18)$$

Finally, the operator Reshape^{-1} is applied

$$\mathcal{H} = \text{Reshape}^{-1}(\mathcal{K}, \mathbb{A}_1, \dots, \mathbb{A}_L) \times_{\mathbb{A}_1} \mathbf{U}^{(1)} \dots \times_{\mathbb{A}_L} \mathbf{U}^{(L)}, \quad (19)$$

which concludes the proof.

Example For a third-order tensor $\mathcal{H} \in \mathbb{C}^{I_1 \times I_2 \times I_3}$ with $\mathbb{A}_1 = \{1, 3\}$, $\mathbb{A}_2 = \{2\}$, the AU-HOSVD will be written as follows:

$$\mathcal{H} = \mathcal{K}_{\mathbb{A}_1/\mathbb{A}_2} \times_{\mathbb{A}_1} \mathbf{U}^{(\mathbb{A}_1)} \times_{\mathbb{A}_2} \mathbf{U}^{(\mathbb{A}_2)}, \quad (20)$$

with $\mathcal{K}_{\mathbb{A}_1/\mathbb{A}_2} \in \mathbb{C}^{I_1 \times I_2 \times I_3}$, $\mathbf{U}^{(\mathbb{A}_1)} \in \mathbb{C}^{I_1 \times I_3 \times I_1}$ and $\mathbf{U}^{(\mathbb{A}_2)} \in \mathbb{C}^{I_2 \times I_2}$.

Remark Let $\mathcal{H} \in \mathbb{C}^{I_1 \times I_2 \times \dots \times I_P \times I_1 \times I_2 \times \dots \times I_P}$ be a $2P$ th-order Hermitian tensor. We consider $2L$ subsets of $\{I_1, \dots, I_P, I_1, \dots, I_P\}$ such as

- $\mathbb{A}_1, \dots, \mathbb{A}_L$ and $\mathbb{A}_{L+1}, \dots, \mathbb{A}_{2L}$ are two partitions of $\{I_1, \dots, I_P\}$
- $\forall l \in [1, L]$, $\mathbb{A}_l = \mathbb{A}_{l+L}$

Under these conditions, the AU-HOSVD of \mathcal{H} is written:

$$\begin{aligned} \mathcal{H} &= \mathcal{K}_{\mathbb{A}_1/\dots/\mathbb{A}_{2L}} \times_{\mathbb{A}_1} \mathbf{U}^{(\mathbb{A}_1)} \dots \times_{\mathbb{A}_L} \mathbf{U}^{(\mathbb{A}_L)} \\ &\quad \times_{\mathbb{A}_{L+1}} \mathbf{U}^{(\mathbb{A}_{L+1})*} \dots \times_{\mathbb{A}_{2L}} \mathbf{U}^{(\mathbb{A}_{2L})*}. \end{aligned}$$

As discussed previously, the main motivation for introducing the new AU-HOSVD is to extract the correlated information when processing the low-rank

decomposition. This is the purpose of the following proposition.

Proposition 3.2 (Low-rank approximation). Let \mathcal{H} , \mathcal{H}_c , \mathcal{H}_0 be three P th-order tensors such that

$$\mathcal{H} = \mathcal{H}_c + \mathcal{H}_0, \quad (21)$$

where \mathcal{H}_c is a $(r_{\mathbb{A}_1}, \dots, r_{\mathbb{A}_L})$ low-rank tensor^c ($r_{\mathbb{A}_l} = \text{rank}([\mathcal{H}_c]_{\mathbb{A}_l})$). Then, \mathcal{H}_0 is approximated by

$$\mathcal{H}_0 \approx \mathcal{H} \times_{\mathbb{A}_1} \mathbf{U}_0^{(\mathbb{A}_1)} \mathbf{U}_0^{(\mathbb{A}_1)H} \dots \times_{\mathbb{A}_L} \mathbf{U}_0^{(\mathbb{A}_L)} \mathbf{U}_0^{(\mathbb{A}_L)H} \quad (22)$$

where $\mathbf{U}_0^{(\mathbb{A}_1)}, \dots, \mathbf{U}_0^{(\mathbb{A}_L)}$ minimize the following criterion:

$$\begin{aligned} &(\mathbf{U}_0^{(\mathbb{A}_1)}, \dots, \mathbf{U}_0^{(\mathbb{A}_L)}) \\ &= \argmin \left\| \mathcal{H}_0 - \mathcal{H} \times_{\mathbb{A}_1} \mathbf{U}_0^{(\mathbb{A}_1)} \mathbf{U}_0^{(\mathbb{A}_1)H} \dots \right. \\ &\quad \left. \times_{\mathbb{A}_L} \mathbf{U}_0^{(\mathbb{A}_L)} \mathbf{U}_0^{(\mathbb{A}_L)H} \right\|^2. \end{aligned} \quad (23)$$

In this paper, the matrices $\mathbf{U}_0^{(\mathbb{A}_l)}$'s are given by truncation of the matrices $\mathbf{U}^{(\mathbb{A}_l)}$'s obtained by the AU-HOSVD $_{\mathbb{A}_1, \dots, \mathbb{A}_L}$ of \mathcal{H} : $\mathbf{U}_0^{(\mathbb{A}_l)} = [\mathbf{u}_{r_{\mathbb{A}_l}+1}^{(\mathbb{A}_l)} \dots \mathbf{u}_{\mathbb{A}_l}^{(\mathbb{A}_l)}]$. This solution is not optimal in the sense of least squares but is easy to implement. However, thanks to the strong link with HOSVD, it should be a correct approximation. That is why iterative algorithms for AU-HOSVD will not be investigated in this paper.

Proof 3.3. By applying Reshape to Equation 21, one obtains

$$\begin{aligned} &\text{Reshape}(\mathcal{H}, \mathbb{A}_1, \dots, \mathbb{A}_L) \\ &= \text{Reshape}(\mathcal{H}_c, \mathbb{A}_1, \dots, \mathbb{A}_L) \\ &\quad + \text{Reshape}(\mathcal{H}_0, \mathbb{A}_1, \dots, \mathbb{A}_L). \end{aligned}$$

Then, $\text{Reshape}(\mathcal{H}_c, \mathbb{A}_1, \dots, \mathbb{A}_L)$ is a $(r_{\mathbb{A}_1}, \dots, r_{\mathbb{A}_L})$ low-rank tensor (where $r_{\mathbb{A}_l} = \text{rank}([\text{Reshape}(\mathcal{H}_c, \mathbb{A}_1, \dots, \mathbb{A}_L)]_l)$). Proposition 2.1 can now be applied, and this leads to

$$\begin{aligned} &\text{Reshape}(\mathcal{H}_0, \mathbb{A}_1, \dots, \mathbb{A}_L) \\ &\approx \text{Reshape}(\mathcal{H}, \mathbb{A}_1, \dots, \mathbb{A}_L) \\ &\quad \times_1 \mathbf{U}_0^{(\mathbb{A}_1)} \mathbf{U}_0^{(\mathbb{A}_1)H} \dots \times_L \mathbf{U}_0^{(\mathbb{A}_L)} \mathbf{U}_0^{(\mathbb{A}_L)H}. \end{aligned}$$

Finally, applying Reshape^{-1} to the previous equation leads to the end of the proof:

$$\mathcal{H}_0 \approx \mathcal{H} \times_{\mathbb{A}_1} \mathbf{U}_0^{(\mathbb{A}_1)} \mathbf{U}_0^{(\mathbb{A}_1)H} \dots \times_{\mathbb{A}_L} \mathbf{U}_0^{(\mathbb{A}_L)} \mathbf{U}_0^{(\mathbb{A}_L)H}.$$

Discussion on choice of partition and complexity As mentioned previously, the total number of AU-HOSVD for a P th-order tensor is equal to B_P . Since this number could become significant, it is important to have a procedure to find good partitions for the AU-HOSVD computation. We propose a two-step procedure. Since the AU-HOSVD has been developed for LR reduction,

the most important criterion is to choose the partitions which emphasize deficient ranks. For some applications, it is possible to use *a priori* knowledge to select some partitions as will be shown in Section 5 for polarimetric STAP. Next, another step is needed if several partitions induce an AU-HOSVD with a deficient rank. At this point, we propose to maximize a criterion (see Section 5.3 for examples) over the remaining partitions.

Concerning the complexity, the number of operation necessary to compute the HOSVD of a P th-order tensor is equal to $4 \left(\prod_p I_p \right) \left(\sum_p I_p \right)$ [3]. Similarly, the complexity of the AU-HOSVD is equal to $4 \left(\prod_p I_p \right) \left(\sum_l I_{\mathbb{A}_l} \right)$.

4 Low-rank filter and detector for multidimensional data based on the alternative unfolding HOSVD

We propose in this section to apply this new decomposition to derive a tensorial LR filter and a tensorial LR detector for multidimensional data. We consider the case of a P -dimensional data \mathcal{X} composed of a target described by its steering tensor \mathcal{S} and two additive noises: \mathcal{N} and \mathcal{C} . We assume that we have K secondary data \mathcal{X}_k containing only the additive noises. This configuration could be summarized as follows:

$$\mathcal{X} = \alpha \mathcal{S} + \mathcal{C} + \mathcal{N} \quad (24)$$

$$\mathcal{X}_k = \mathcal{C}_k + \mathcal{N}_k \quad k \in [1, K]. \quad (25)$$

where $\mathcal{X}, \mathcal{X}_k, \mathcal{C}, \mathcal{C}_k, \mathcal{N}, \mathcal{N}_k \in \mathbb{C}^{I_1 \times \dots \times I_P}$. We assume that $\mathcal{N}, \mathcal{N}_k \sim \mathcal{CN}(\mathbf{0}, \sigma^2 \text{SqMat}^{-1}(\mathbf{I}_{1 \dots I_P}))$ and $\mathcal{C}, \mathcal{C}_k \sim \mathcal{CN}(\mathbf{0}, \mathcal{R}_c)$ ($\text{SqMat}^{-1}(\mathbf{I}_{1 \dots I_P}), \mathcal{R}_c \in \mathbb{C}^{I_1 \times \dots \times I_P \times I_1 \times \dots \times I_P}$). These notations mean $\text{vec}(\mathcal{N}), \text{vec}(\mathcal{N}_k) \sim \mathcal{CN}(\mathbf{0}, \sigma^2 \mathbf{I}_{I_1 \dots I_P})$ and $\text{vec}(\mathcal{C}), \text{vec}(\mathcal{C}_k) \sim \mathcal{CN}(\mathbf{0}, \text{SqMat}(\mathcal{R}_c))$. We denote $\mathcal{R} = \mathcal{R}_c + \sigma^2 \text{SqMat}^{-1}(\mathbf{I}_{1 \dots I_P})$ the covariance tensor of the total interference. We assume in the following that the additive noise \mathcal{C} (and hence also \mathcal{C}_k) has a low-rank structure.

4.1 LR filters

Proposition 4.1 (Optimal tensor filter). *The optimal tensor filter, \mathcal{W} , is defined as the filter which maximizes the SINR output*

$$\text{SINR}_{\text{out}} = \frac{|\langle \mathcal{W}, \mathcal{S} \rangle|^2}{\text{vec}(\mathcal{W})^H \text{SqMat}(\mathcal{R}) \text{vec}(\mathcal{W})}. \quad (26)$$

It is given by the following expression:

$$\mathcal{W}_{\text{opt}} = \text{vec}^{-1} \left(\text{SqMat}(\mathcal{R})^{-1} \text{vec}(\mathcal{S}) \right). \quad (27)$$

Proof 4.1. See Appendix 1.

In practical cases, \mathcal{R} is unknown. Hence, we propose an adaptive version:

$$\hat{\mathcal{W}}_{\text{opt}} = \text{vec}^{-1} \left(\text{SqMat}(\hat{\mathcal{R}})^{-1} \text{vec}(\mathcal{S}) \right), \quad (28)$$

where $\hat{\mathcal{R}}$ is the estimation of \mathcal{R} given by the SCT from Equation 9. This filter is equivalent to the vector filter. In order to reach correct performance [29], $K = 2I_1 \dots I_P$ secondary data are necessary. As with the vectorial approach, it is interesting to use the low-rank structure of \mathcal{C} to reduce this number K .

Proposition 4.2 (Low-rank tensor filter). *Let $\mathbb{A}_1, \dots, \mathbb{A}_L$ be a partition of $\{1, \dots, P\}$. The low-rank tensor filter associated to AU-HOSVD $_{\mathbb{A}_1, \dots, \mathbb{A}_L}$, which removes the low-rank noise \mathcal{C} , is given by*

$$\mathcal{W}_{lr(\mathbb{A}_1, \dots, \mathbb{A}_P)} = \mathcal{S} \times_{\mathbb{A}_1} \mathbf{U}_0^{(\mathbb{A}_1)} \mathbf{U}_0^{(\mathbb{A}_1)H} \dots \times_{\mathbb{A}_L} \mathbf{U}_0^{(\mathbb{A}_L)} \mathbf{U}_0^{(\mathbb{A}_L)H} \quad (29)$$

$$y = |\langle \mathcal{W}_{\mathbb{A}_1, \dots, \mathbb{A}_P}, \mathcal{X} \rangle|. \quad (30)$$

The matrices $\mathbf{U}_0^{(\mathbb{A}_l)}$'s are given by truncation of the matrices $\mathbf{U}^{(\mathbb{A}_l)}$'s obtained by the AU-HOSVD $_{\mathbb{A}_1, \dots, \mathbb{A}_L}$ of \mathcal{R} : $\mathbf{U}_0^{(\mathbb{A}_l)} = [\mathbf{u}_{r_{\mathbb{A}_l}+1}^{(\mathbb{A}_l)} \dots \mathbf{u}_{\mathbb{A}_l}^{(\mathbb{A}_l)}]$.

For a P -dimensional configuration, B_P filters will be obtained.

Proof 4.2. See Appendix 2.

In its adaptive version, denoted $\hat{\mathcal{W}}_{lr(\mathbb{A}_1/\dots/\mathbb{A}_L)}$, the matrices $\mathbf{U}_0^{(\mathbb{A}_1)}, \dots, \mathbf{U}_0^{(\mathbb{A}_L)}$ are replaced by their estimates $\hat{\mathbf{U}}_0^{(\mathbb{A}_1)}, \dots, \hat{\mathbf{U}}_0^{(\mathbb{A}_L)}$.

The number of secondary data necessary to reach classical performance is not known. In the vectorial case, the performance of LR filter depends on the deficient rank [10,11]. It will be similar for the LR tensor filters. This implies that the choice of the partition $\mathbb{A}_1, \dots, \mathbb{A}_L$ is critical.

4.2 LR detectors

In a detection point of view, the problem can also be stated as the following binary hypothesis test:

$$\begin{cases} H_0 : \mathcal{X} = \mathcal{C} + \mathcal{N}, \mathcal{X}_k = \mathcal{C}_k + \mathcal{N}_k, k \in [1, K] \\ H_1 : \mathcal{X} = \alpha \mathcal{S} + \mathcal{C} + \mathcal{N}, \mathcal{X}_k = \mathcal{C}_k + \mathcal{N}_k, k \in [1, K]. \end{cases} \quad (31)$$

Table 1 Description of the LR filters and LR detectors provided by AU-HOSVD for polarimetric STAP

Partition	Filters	Detectors	Ranks	Methods
$\mathbb{A}_1 = \{1, 2, 3\}$	$\hat{\mathcal{W}}_{lr(1,2,3)}$	$\hat{\Lambda}_{(1,2,3)}$	r_{123}	Vector
$\mathbb{A}_1 = \{1\}, \mathbb{A}_2 = \{2\}, \mathbb{A}_3 = \{3\}$	$\hat{\mathcal{W}}_{lr(1/2/3)}$	$\hat{\Lambda}_{(1/2/3)}$	r_1, r_2, r_3	HOSVD
$\mathbb{A}_1 = \{1, 2\}, \mathbb{A}_2 = \{3\}$	$\hat{\mathcal{W}}_{lr(1,2/3)}$	$\hat{\Lambda}_{(1,2/3)}$	r_{12}, r_3	AU-HOSVD
$\mathbb{A}_1 = \{1\}, \mathbb{A}_2 = \{2, 3\}$	$\hat{\mathcal{W}}_{lr(1/2,3)}$	$\hat{\Lambda}_{(1/2,3)}$	r_1, r_{23}	AU-HOSVD
$\mathbb{A}_1 = \{1, 3\}, \mathbb{A}_2 = \{2\}$	$\hat{\mathcal{W}}_{lr(1,3/2)}$	$\hat{\Lambda}_{(1,3/2)}$	r_{13}, r_2	AU-HOSVD

Table 2 Summary of the value of the ranks for the two scenarios: $\rho = 1, \rho = 0.5$

	r_1	r_2	r_3	r_{12}	r_{23}	r_{13}	r_{123}
$\rho = 1$	Full	Full	2	15	16	16	30
$\rho = 0.5$	Full	Full	Full	15	Full	Full	45

Proposition 4.3 (Low-rank tensor detector). Let $\mathbb{A}_1, \dots, \mathbb{A}_L$ be a partition of $\{1, \dots, P\}$. The low-rank tensor detector associated to AU-HOSVD $_{\mathbb{A}_1, \dots, \mathbb{A}_L}$, which removes the low-rank noise \mathcal{C} and performs the generalized likelihood ratio test (GLRT), is given by

$$\Lambda_{\mathbb{A}_1 \dots \mathbb{A}_L} = \frac{|\langle \mathcal{S}_{\mathbb{A}_1 \dots \mathbb{A}_L}, \mathcal{X}_{\mathbb{A}_1 \dots \mathbb{A}_L} \rangle|^2}{\langle \mathcal{S}_{\mathbb{A}_1 \dots \mathbb{A}_L}, \mathcal{S}_{\mathbb{A}_1 \dots \mathbb{A}_L} \rangle \langle \mathcal{X}_{\mathbb{A}_1 \dots \mathbb{A}_L}, \mathcal{X}_{\mathbb{A}_1 \dots \mathbb{A}_L} \rangle} \quad (32)$$

where

$$\begin{aligned} \mathcal{X}_{\mathbb{A}_1 \dots \mathbb{A}_L} &= \mathcal{X} \times_{\mathbb{A}_1} \mathbf{U}_0^{(\mathbb{A}_1)} \mathbf{U}_0^{(\mathbb{A}_1)H} \dots \times_{\mathbb{A}_L} \mathbf{U}_0^{(\mathbb{A}_L)} \mathbf{U}_0^{(\mathbb{A}_L)H} \\ \mathcal{S}_{\mathbb{A}_1 \dots \mathbb{A}_L} &= \mathcal{S} \times_{\mathbb{A}_1} \mathbf{U}_0^{(\mathbb{A}_1)} \mathbf{U}_0^{(\mathbb{A}_1)H} \dots \times_{\mathbb{A}_L} \mathbf{U}_0^{(\mathbb{A}_L)} \mathbf{U}_0^{(\mathbb{A}_L)H} \end{aligned} \quad (33)$$

The matrices $\mathbf{U}_0^{(\mathbb{A}_l)}$'s are given by truncation of the matrices $\mathbf{U}^{(\mathbb{A}_l)}$'s obtained by the AU-HOSVD $_{\mathbb{A}_1, \dots, \mathbb{A}_L}$ of \mathcal{R} : $\mathbf{U}_0^{(\mathbb{A}_l)} = [\mathbf{u}_{r_{\mathbb{A}_l}+1}^{(\mathbb{A}_l)} \dots \mathbf{u}_{\mathbb{A}_l}^{(\mathbb{A}_l)}]$.

Proof 4.3. See Appendix 3.

In its adaptive version, denoted as $\hat{\Lambda}_{\mathbb{A}_1 \dots \mathbb{A}_L}$, the matrices $\mathbf{U}_0^{(\mathbb{A}_1)}, \dots, \mathbf{U}_0^{(\mathbb{A}_L)}$ are replaced by their estimates $\hat{\mathbf{U}}_0^{(\mathbb{A}_1)}, \dots, \hat{\mathbf{U}}_0^{(\mathbb{A}_L)}$.

4.3 Particular case

When the partition $\mathbb{A}_1 = \{1, \dots, P\}$ is chosen, the filter and the detector obtained by the AU-HOSVD are equal to the vectorial one. In other words, it is equivalent to apply the operator *vec* on Equations 24 and 25 and use the vectorial method. We denote $m = I_1 \dots I_P$, $\mathbf{x} = \text{vec}(\mathcal{X})$ and $\mathbf{s} = \text{vec}(\mathcal{S})$. We obtain the basis of the orthogonal clutter subspace \mathbf{U}_0 by taking the last $(m-r)$ columns of \mathbf{U} which is computed by the SVD of $\text{SqMat}(\mathcal{R}) = \mathbf{U}\Sigma\mathbf{V}^H$. From this basis, the low-rank filter is then equal to [10,11]:

$$\mathbf{w}_{lr} = \mathbf{U}_0 \mathbf{U}_0^H \mathbf{s}, \quad (34)$$

$$y_{lr} = |\langle \mathbf{w}_{lr}, \mathbf{x} \rangle|. \quad (35)$$

In its adaptive version, denoted $\hat{\mathbf{w}}_{lr}$, the matrix \mathbf{U}_0 is replaced by its estimate $\hat{\mathbf{U}}_0$.

Similarly, the detector is equal to the low-rank normalized matched filter proposed in [30,31]:

$$\Lambda_{\text{LR-NMF}} = \frac{|\mathbf{s}^H \mathbf{U}_0 \mathbf{U}_0^H \mathbf{x}|^2}{(\mathbf{s}^H \mathbf{U}_0 \mathbf{U}_0^H \mathbf{s})(\mathbf{x}^H \mathbf{U}_0 \mathbf{U}_0^H \mathbf{x})}. \quad (36)$$

In its adaptive version, denoted $\hat{\Lambda}_{\text{LR-NMF}}$, the matrix \mathbf{U}_0 is replaced by its estimate $\hat{\mathbf{U}}_0$.

5 Application to polarimetric STAP

5.1 Model

We propose to apply the LR filters and the LR detectors derived in the previous section to polarimetric STAP. STAP is applied to airborne radar in order to detect moving targets [20]. Typically, the radar receiver consists of an array of N antenna elements processing M pulses in a coherent processing interval. In polarimetric configuration, each element transmits and receives in both H and V polarizations, resulting in three polarimetric channels (HH, VV, HV/VH). The number of dimensions of polarimetric STAP data is then equal to three: N antenna, M pulses, and three polarimetric channels.

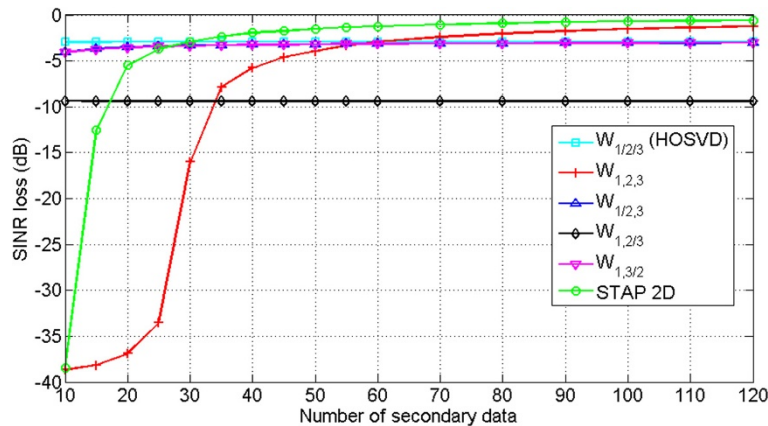


Figure 1 SINR losses versus K for $\rho = 1$, $\text{CNR} = 40$ dB. Target located at position $(\theta = 0^\circ, \nu = 10 \text{ m s}^{-1})$.

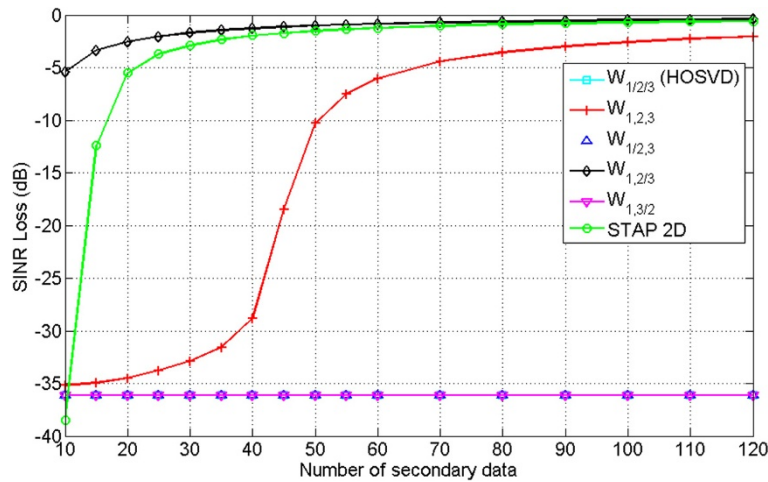


Figure 2 SINR losses versus K for $\rho = 0.5$, $\text{CNR} = 40$ dB. Target located at position $(\theta = 0^\circ, v = 10 \text{ m s}^{-1})$.

We are in the data configuration proposed in Equations 24 and 25 which is recalled in the following equations:

$$\mathcal{X} = \alpha \mathcal{S} + \mathcal{C} + \mathcal{N} \quad (37)$$

$$\mathcal{X}_k = \mathcal{C}_k + \mathcal{N}_k \quad k \in [1, K], \quad (38)$$

where $\mathcal{X}, \mathcal{X}_k \in \mathbb{C}^{M \times N \times 3}$. The steering tensor \mathcal{S} and the responses of the background \mathcal{C} and \mathcal{C}_k , called *clutter* in STAP, are obtained from the model proposed in [22]. \mathcal{N} and \mathcal{N}_k , which arise from the electrical components of the radar, are distributed as a white Gaussian noise.

The steering tensor, \mathcal{S} , is formed as follows:

$$\mathcal{S}(\theta, v) = \text{vec}^{-1} \begin{pmatrix} \mathbf{s}_{\text{HH}}(\theta, v) \\ \alpha_{\text{VV}} \mathbf{s}_{\text{HH}}(\theta, v) \\ \alpha_{\text{VH}} \mathbf{s}_{\text{HH}}(\theta, v) \end{pmatrix}, \quad (39)$$

where $\mathbf{s}_{\text{HH}}(\theta, v)$ is the 2D steering vector [20], characterized by the angle of arrival (AOA) θ and the speed v of the target. α_{VV} and α_{VH} are two complex coefficients. These coefficients are assumed to be known. This is the

case when the detection process concerns a particular target (surface, double-bounds, volume, ...). The covariance tensor, denoted as $\mathcal{R} \in \mathbb{C}^{M \times N \times 3 \times M \times N \times 3}$, of the two noises ($\mathcal{C} + \mathcal{N}$ and $\mathcal{C}_k + \mathcal{N}_k$) is given by

$$\mathcal{R} = \text{SqMat}^{-1} (\mathbf{R}_{pc} + \sigma^2 \mathbf{I}_{3MN}), \quad (40)$$

where σ^2 is the power of the white noise. \mathbf{R}_{pc} is built as follows:

$$\mathbf{R}_{pc} = \begin{pmatrix} \mathbf{R}_c & \rho \sqrt{\gamma_{\text{VV}}} \mathbf{R}_c & \mathbf{0} \\ \rho^* \sqrt{\gamma_{\text{VV}}} \mathbf{R}_c & \gamma_{\text{VV}} \mathbf{R}_c & \mathbf{0} \\ \mathbf{0} & \mathbf{0} & \gamma_{\text{VH}} \mathbf{R}_c \end{pmatrix}, \quad (41)$$

where $\mathbf{R}_c \in \mathbb{C}^{MN \times MN}$ is the covariance matrix of the HH channel *clutter*, built as the 2D clutter, which is known to have a LR structure [20]. γ_{VV} and γ_{VH} are two coefficients relative to the nature of the ground, and ρ is the correlation coefficient between the channels HH and VV. Due to the structure of \mathbf{R}_{pc} , the low-rank structure of the clutter is preserved.

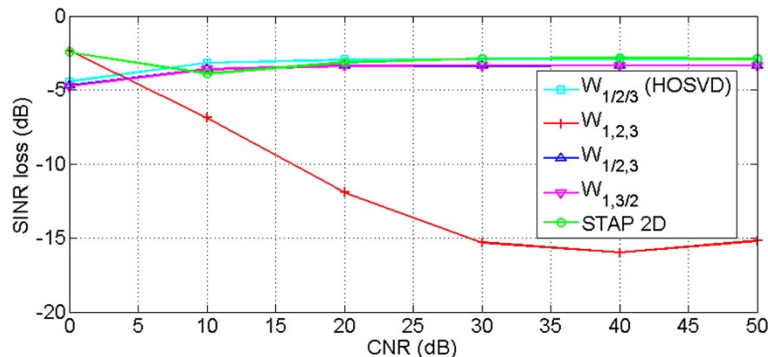


Figure 3 SINR losses versus CNR for $\rho = 1$, $K = 30$, $N_{\text{rea}} = 1,000$. Target located at $(\theta = 0^\circ, v = 10 \text{ m s}^{-1})$.

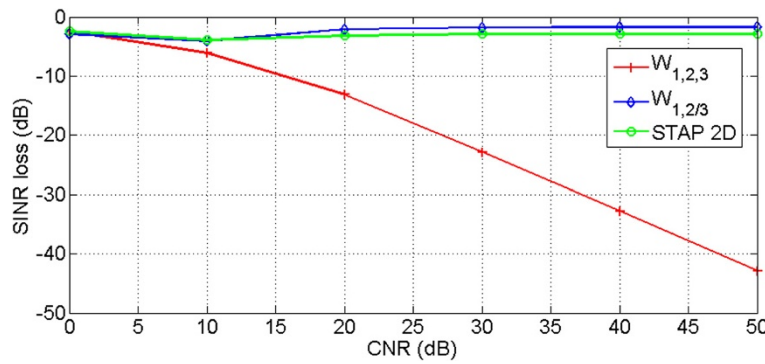


Figure 4 SINR losses versus CNR for $\rho = 0.5$, $K = 30$, $N_{rea} = 1,000$. Target located at $(\theta = 0^\circ, v = 10 \text{ m s}^{-1})$.

In the following subsection, we discuss about the choice of partitions in this particular context.

5.2 Choice of partition \mathbb{A}

For polarimetric STAP, we have $P = 3$ and $\mathbb{A} = \{1, 2, 3\}$: $B_3 = 5$ LR filters and LR detectors are obtained. The different choices of partition are presented in Table 1. All filters and detectors are computed with the AU-HOSVD. Nevertheless, the first two partitions are particular cases. When $\mathbb{A}_1 = \{1, 2, 3\}$, the algorithms are equal to the vectorial one as mentioned in Section 4.3. When $\mathbb{A}_1 = \{1\}$, $\mathbb{A}_2 = \{2\}$, $\mathbb{A}_3 = \{3\}$, we obtain the same LR filter and LR detector as those given by the HOSVD. The ranks relative to the LR filters and LR detectors are described in the following:

- The rank r_1 is the spatial rank, and the rank r_2 is the temporal rank. They depend on radar parameters, and in most cases, they are not deficient.
- r_3 could be deficient depending on the nature of the data and especially on the correlation coefficient ρ between the polarimetric channels.

- r_{12} is the same as the 2D low-rank vector case and can be calculated by the Brennan's rule [21].
- r_{123} is deficient and is linked to r_3 and r_{12} .
- r_{13} and r_{23} could be deficient and depends on r_1 , r_2 and r_3 .

5.3 Performance criteria

In order to evaluate the performance of our LR filters, we evaluate the SINR loss defined as follows [20]:

$$\rho_{\text{loss}} = \frac{\text{SINR}_{\text{out}}}{\text{SINR}_{\text{max}}}, \quad (42)$$

where SINR_{out} is the SINR at the output of the LR tensor STAP filter and SINR_{max} the SINR at the output of the optimal filter \mathbf{W}_{opt} . The SINR_{out} is maximum when $\mathbf{W} = \mathbf{W}_{\text{opt}} = \text{vec}^{-1}(\text{SqMat}(\mathcal{R})^{-1} \text{vec}(\mathcal{S}))$. After some developments, the SINR loss is equal to [1]

$$\rho_{\text{loss}} = \frac{|(\text{vec}(\mathbf{W}_{lr})^H \text{vec}(\mathcal{S}))|^2}{\text{vec}(\mathbf{W}_{lr})^H \text{SqMat}(\mathcal{R}) \text{vec}(\mathbf{W}_{lr}) \text{vec}(\mathcal{S})^H \text{SqMat}(\mathcal{R})^{-1} \text{vec}(\mathcal{S})}. \quad (43)$$

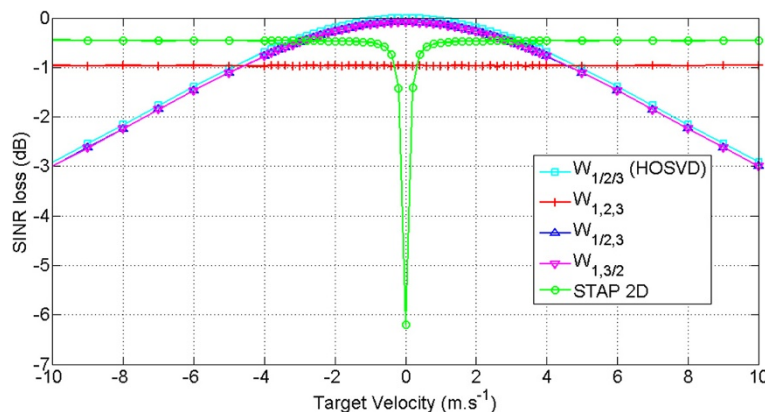


Figure 5 SINR losses versus target velocity for $\rho = 1$, $\text{CNR} = 40 \text{ dB}$, $K = 180$, $N_{rea} = 1,000$. Target located at $\theta = 0^\circ$.

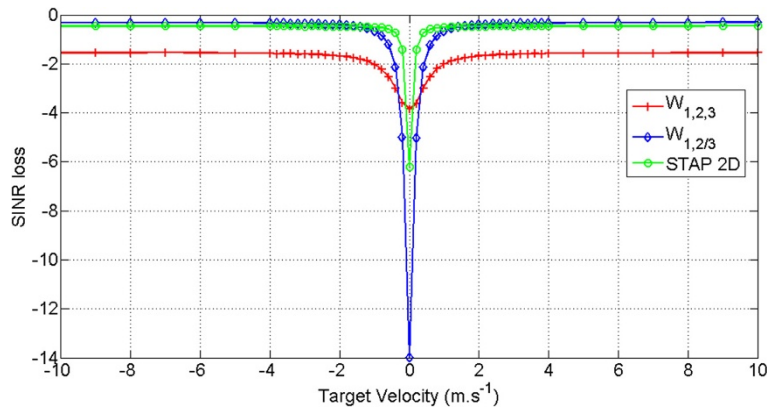


Figure 6 SINR losses versus target velocity for $\rho = 0.5$, $\text{CNR} = 40$ dB, $K = 180$, $N_{\text{rea}} = 1,000$. Target located at $\theta = 0^\circ$.

For the moment, as the analytical formulation of the SINR loss for the tensorial approach is not available, it will be evaluated using Monte Carlo simulations.

In order to evaluate the performance of our LR detectors, we use the probability of false alarm (Pfa) and probability of detection (Pd):

$$\text{Pfa} = \Pr(\hat{\Lambda}_{A_1 \dots A_L} > \eta/H_0) \quad (44)$$

$$\text{Pd} = \Pr(\hat{\Lambda}_{A_1 \dots A_L} > \eta/H_1), \quad (45)$$

where η is the detector threshold. Since there is no analytical formulation for Pfa and Pd (for the adaptive version) even in the vectorial case, Monte Carlo simulations are used to evaluate them.

5.4 Simulations

Parameters The simulations are performed with the following parameters. The target is characterized by an angle

of arrival (AOA) of $\theta = 0^\circ$ and a speed of $v = 10 \text{ m s}^{-1}$, a case where the 2D STAP is known to be inefficient because the target is close to the clutter ridge. The radar receiver contains $N = 8$ sensors processing $M = 8$ pulses. The platform speed V , is equal to 100 m s^{-1} . For the clutter, we consider two cases: $\rho = 1$, i.e., the channels HH and VV are entirely correlated and $\rho = 0.5$. The SNR is equal to 45 dB and the clutter-to-noise ratio (CNR) to 40 dB. r_1 , r_2 , r_3 , and r_{12} can be calculated based on the radar configuration. r_{13} depends on the value of ρ . r_{123} and r_{23} are estimated according to the singular values of the different unfoldings of \mathcal{R} . The results are presented in Table 2. All Monte-Carlo simulations are performed with $N_{\text{rea}} = 1,000$ samples, except the probability of false alarm where $N_{\text{rea}} = 100$.

Results on SINR losses Figures 1 and 2 show the SINR losses for each filter as a function of K . SINR losses are obtained from Monte-Carlo simulations using Equation 43. On both figures, the SINR loss of the

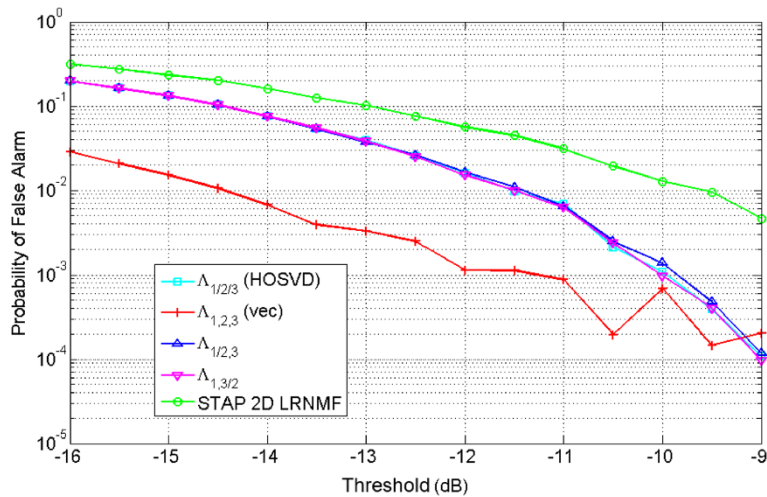


Figure 7 Pfa versus threshold for $\rho = 1$, $K = 30$, $\text{CNR} = 40$ dB, $N_{\text{rea}} = 100$.

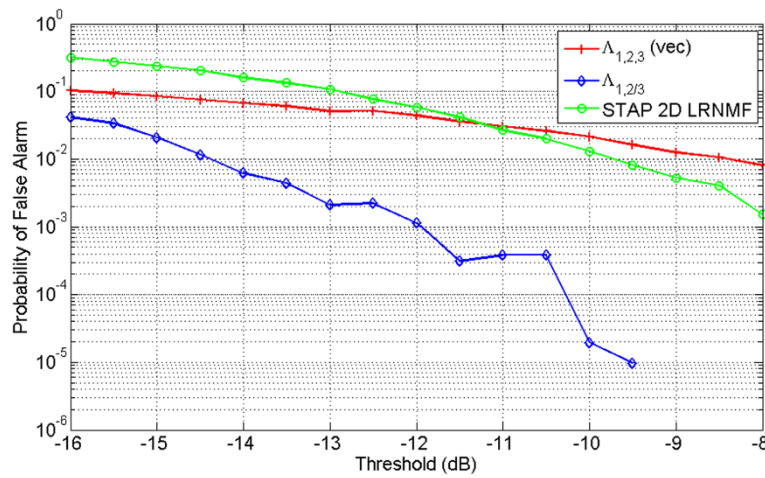


Figure 8 Pfa versus threshold for $\rho = 0.5$, $K = 30$, $\text{CNR} = 40$ dB, $N_{\text{rea}} = 100$.

2D STAP is plotted for comparison. The well-known result is obtained: the SINR loss reaches -3 dB when $K = 2r_{12} = 30$, and it tends to 0 dB as K increases. Similarly, the SINR loss of $\hat{\mathbf{W}}_{lr(1,2,3)}$ reaches -3 dB when $K = 2r_{123}$ (60 for $\rho = 1$ and 90 for $\rho = 0.5$). When $\rho = 1$, all LR filters achieve reasonable performance since all ranks, except r_1 and r_2 , are deficient. $\hat{\mathbf{W}}_{lr(1/2/3)}$, $\hat{\mathbf{W}}_{lr(1/2,3)}$, and $\hat{\mathbf{W}}_{lr(1,3/2)}$, which can only be obtained by AU-HOSVD, outperform $\hat{\mathbf{W}}_{lr(1,2,3)}$ and the 2D STAP for a small number of secondary data. This situation is more realistic since the assumption of homogeneity of the data is no longer true when K is too large. $\hat{\mathbf{W}}_{lr(1,2/3)}$ has poor performance in this scenario.

When $\rho = 0.5$, $\hat{\mathbf{W}}_{lr(1,2/3)}$ outperforms $\hat{\mathbf{W}}_{lr(1,2,3)}$ and the 2D STAP regardless of the number of secondary data. This

corresponds to a more realistic scenario, since the channels HH and VV are not entirely correlated. $\hat{\mathbf{W}}_{lr(1/2/3)}$, $\hat{\mathbf{W}}_{lr(1/2,3)}$, and $\hat{\mathbf{W}}_{lr(1,3/2)}$ do not have acceptable performance. This is explained by the fact that all ranks pertaining to these filters are full and no projection can be done as mentioned at the end of Section 3. These filters (for $\rho = 0.5$) will not be studied in the rest of the simulations.

Figures 3 and 4 show the SINR loss as a function of the CNR for $K = 2r_{12} = 30$ secondary data. They show that our filters are more robust than the vectorial one for polarimetric STAP configuration.

Figures 5 and 6 show the SINR loss as a function of the target velocity for $K = 180$. For both cases, the 2D STAP achieves the expected performance. For $\rho = 1$, the difference in polarimetric properties between the target and

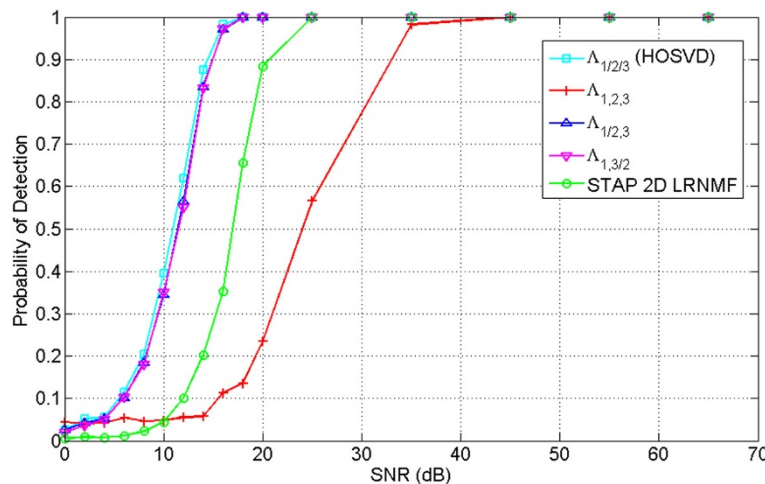


Figure 9 Pd versus SNR for $\rho = 1$, $K = 30$, $\text{CNR} = 40$ dB, $\text{Pfa} = 10^{-2}$, $N_{\text{rea}} = 1,000$. Target located at position ($\theta = 0^\circ$, $v = 10$ m s $^{-1}$).

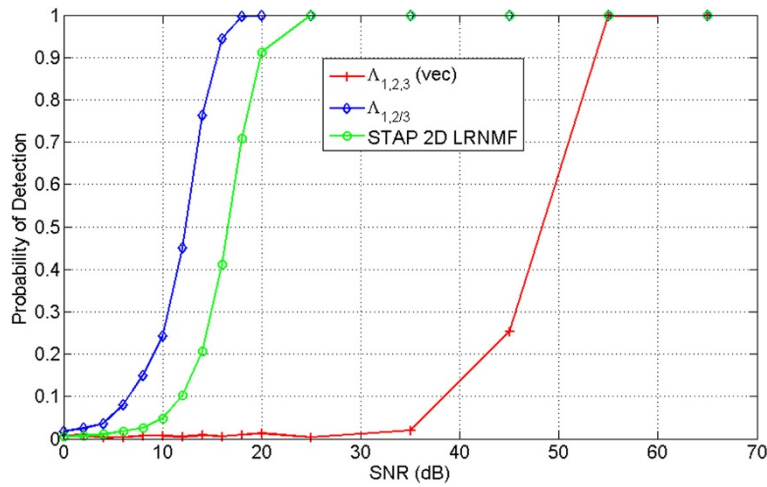


Figure 10 Pd versus SNR for $\rho = 0.5$, $K = 30$, $\text{CNR} = 40$ dB, $\text{Pfa} = 10^{-2}$, $N_{\text{rea}} = 1,000$. Target located at position $(\theta = 0^\circ, v = 10 \text{ m s}^{-1})$.

the clutter is exploited by our filters, since r_3 is deficient. When the target is in the clutter ridge, the SINR loss is higher (especially for $\hat{\mathbf{W}}_{lr(1/2/3)}$, $\hat{\mathbf{W}}_{lr(1/2,3)}$, and $\hat{\mathbf{W}}_{lr(1,3/2)}$) than the 2D LR STAP filter. By contrast, when $\rho = 0.5$, the 2D LR STAP filter outperforms $\hat{\mathbf{W}}_{lr(1,2/3)}$ $\hat{\mathbf{W}}_{lr(1,2,3)}$ (in the context of large K), since r_3 is full.

Results on Pfa and Pd The Pfa as a function of threshold is presented in Figures 7 and 8. The probability of detection as a function of SNR is presented in Figures 9 and 10 for $K = 30$. The thresholds are chosen in order to have a Pfa of 10^{-2} according to Figures 7 and 8. When $\rho = 1$, $\hat{\Lambda}_{lr(1/2/3)}$, $\hat{\Lambda}_{lr(1/2,3)}$, and $\hat{\Lambda}_{lr(1,3/2)}$, which can only be obtained by AU-HOSVD, outperform $\hat{\Lambda}_{lr(1,2,3)}$ and the 2D STAP LRNMF. For instance, Pd is equal to 90% when the SNR is equal to 15 dB for $\hat{\Lambda}_{lr(1/2/3)}$, $\hat{\Lambda}_{lr(1/2,3)}$, and $\hat{\Lambda}_{lr(1,3/2)}$; 20 dB for the 2D STAP LRNMF; and 33 dB for $\hat{\Lambda}_{lr(1,2,3)}$. When $\rho = 0.5$, $\hat{\Lambda}_{lr(1,2/3)}$ outperforms $\hat{\Lambda}_{lr(1,2,3)}$ and the 2D STAP LRNMF. For instance, Pd is equal to 90% when the SNR is equal to 16 dB for $\hat{\Lambda}_{lr(1,2/3)}$, 20 dB for the 2D STAP LRNMF, and 54 dB for $\hat{\Lambda}_{lr(1,2,3)}$.

The results on Pd confirm the results on SINR loss concerning the most efficient partition for the two scenarios. In particular, it shows that the best results are provided by the filters and detectors which can only be obtained with the AU-HOSVD.

6 Conclusion

In this paper, we introduced a new multilinear decomposition: the AU-HOSVD. This new decomposition generalizes the HOSVD and highlights the correlated data in a multidimensional set. We showed that the properties of the AU-HOSVD are proven to be the same as those for HOSVD: the orthogonality and the LR decomposition. We have also derived LR filters and LR detectors based on

AU-HOSVD for multidimensional data containing one LR structure contribution. Finally, we applied our new LR filters and LR detectors to polarimetric space-time adaptive processing (STAP) where the dimension of the problem is three and the contribution of the background is correlated in time and space. Simulations based on signal-to-interference-plus-noise ratio (SINR) losses, probability of detection (Pd), and probability of false alarm (Pfa) showed the interest of our approach: LR filters and LR detectors which can be obtained only from AU-HOSVD outperformed the vectorial approach and those obtained from HOSVD in the general polarimetry physic model (where the channels HH and VV are not completely correlated). The main future work concerns the application of the LR filters and LR detectors developed from the AU-HOSVD for the general system of MIMO-STAP [23-26].

Endnotes

^a This new decomposition has similarity with the block term decomposition introduced in [13,32] and [33], which proposes to unify HOSVD and CP.

^b Using this assumption, a low-rank vector STAP filter can be derived based on the projector onto the subspace orthogonal to the clutter (see [10,11,34] for more details).

^c This definition of rank is directly extended from the definition of p -ranks.

Appendices

Appendix 1

Proof of Proposition 4.1

By analogy with the vector case [35], we derive the optimal filter \mathbf{W}_{opt} , which maximizes the output SINR_{out} :

$$\text{SINR}_{\text{out}} = \frac{|\langle \mathbf{W}_{\text{opt}}, \mathbf{S} \rangle|^2}{\text{vec}(\mathbf{W}_{\text{opt}})^H \text{SqMat}(\mathcal{R}) \text{vec}(\mathbf{W}_{\text{opt}})}. \quad (46)$$

Then,

$$\begin{aligned}
 & | \langle \mathbf{W}_{\text{opt}}, \mathbf{S} \rangle |^2 \\
 &= \left| \text{vec}(\mathbf{W}_{\text{opt}})^H \text{vec}(\mathbf{S}) \right|^2 \\
 &= \left| \text{vec}(\mathbf{W}_{\text{opt}})^H \text{SqMat}(\mathcal{R})^{\frac{1}{2}} \text{SqMat}(\mathcal{R})^{-\frac{1}{2}} \text{vec}(\mathbf{S}) \right|^2 \\
 &= \left| \langle \text{SqMat}(\mathcal{R})^{\frac{1}{2}(H)} \text{vec}(\mathbf{W}_{\text{opt}}), \text{SqMat}(\mathcal{R})^{-\frac{1}{2}} \text{vec}(\mathbf{S}) \rangle \right|^2
 \end{aligned} \quad (47)$$

By Cauchy-Schwarz inequality, (47) is maximum when $\text{SqMat}(\mathcal{R})^{\frac{1}{2}(H)} \text{vec}(\mathbf{W}_{\text{opt}}) = \text{SqMat}(\mathcal{R})^{-\frac{1}{2}} \text{vec}(\mathbf{S})$ and $\text{vec}(\mathbf{W}_{\text{opt}}) = \text{SqMat}(\mathcal{R})^{-1} \text{vec}(\mathbf{S})$. We replace \mathbf{W}_{opt} in (46):

$$\begin{aligned}
 x' \text{SINR} &= \frac{|\text{vec}(\mathbf{S})^H \text{SqMat}(\mathcal{R})^{-1} \text{vec}(\mathbf{S})|^2}{\text{vec}(\mathbf{S})^H \text{SqMat}(\mathcal{R})^{-1} \text{SqMat}(\mathcal{R}) \text{SqMat}(\mathcal{R})^{-1} \text{vec}(\mathbf{S})} \\
 &= |\text{vec}(\mathbf{S})^H \text{SqMat}(\mathcal{R})^{-1} \text{vec}(\mathbf{S})| \\
 &= \text{SINR}_{\text{max}}
 \end{aligned} \quad (48)$$

Appendix 2

Proof of Proposition 4.2

We propose to derive the low-rank tensor filter as follows:

- First, the covariance tensor \mathcal{R} is decomposed with the AU-HOSVD:

$$\mathcal{R} = \mathcal{K}_{\mathbb{A}_1/\dots/\mathbb{A}_{2L}} \times_{\mathbb{A}_1} \mathbf{U}^{(\mathbb{A}_1)} \dots \times_{\mathbb{A}_L} \mathbf{U}^{(\mathbb{A}_L)} \times_{\mathbb{A}_{L+1}} \mathbf{U}^{(\mathbb{A}_1)*} \dots \times_{\mathbb{A}_{2L}} \mathbf{U}^{(\mathbb{A}_L)*}. \quad (49)$$

- $r_{\mathbb{A}_1}, \dots, r_{\mathbb{A}_L}$ ($r_{\mathbb{A}_l} = \text{rank}([\mathcal{R}]_{\mathbb{A}_l})$) are estimated.
- Each $\mathbf{U}^{(\mathbb{A}_l)}$ is truncated to obtain

$$\mathbf{U}_0^{(\mathbb{A}_l)} = [\mathbf{u}_{r_{\mathbb{A}_l}+1}^{(\mathbb{A}_l)}, \dots, \mathbf{u}_{\mathbb{A}_l}^{(\mathbb{A}_l)}].$$

- Proposition 3.2, with $\mathcal{H} = \mathcal{X}$, $\mathcal{H}_c = \mathcal{C}$ and $\mathcal{H}_0 = \alpha \mathbf{S} + \mathcal{N}$ is applied in order to remove the LR contribution:

$$\mathcal{X} \times_{\mathbb{A}_1} \mathbf{U}_0^{(\mathbb{A}_1)} \mathbf{U}_0^{(\mathbb{A}_1)H} \dots \times_{\mathbb{A}_L} \mathbf{U}_0^{(\mathbb{A}_L)} \mathbf{U}_0^{(\mathbb{A}_L)H} \approx \alpha \mathbf{S} + \mathcal{N}. \quad (50)$$

- The problem is then to filter \mathbf{S} which is corrupted by a white noise \mathcal{N} . The filter given by (27) is applied with $\mathcal{R} = \mathcal{J}_{I_1 \dots I_p}$:

$$y = \left| \langle \mathbf{S}, \mathcal{X} \times_{\mathbb{A}_1} \mathbf{U}_0^{(\mathbb{A}_1)} \mathbf{U}_0^{(\mathbb{A}_1)H} \dots \times_{\mathbb{A}_L} \mathbf{U}_0^{(\mathbb{A}_L)} \mathbf{U}_0^{(\mathbb{A}_L)H} \rangle \right|. \quad (51)$$

- Finally, the output filter is rewritten:

$$\mathcal{W}_{lr(\mathbb{A}_1, \dots, \mathbb{A}_p)} = \mathbf{S} \times_{\mathbb{A}_1} \mathbf{U}_0^{(\mathbb{A}_1)} \mathbf{U}_0^{(\mathbb{A}_1)H} \dots \times_{\mathbb{A}_L} \mathbf{U}_0^{(\mathbb{A}_L)} \mathbf{U}_0^{(\mathbb{A}_L)H} \quad (52)$$

$$y = \left| \langle \mathcal{W}_{\mathbb{A}_1, \dots, \mathbb{A}_p}, \mathcal{X} \rangle \right|. \quad (53)$$

Appendix 3

Proof of Proposition 4.3

To prove Proposition 4.3, let us recall the hypothesis test:

$$\begin{cases} H_0 : \mathcal{X} = \mathcal{C} + \mathcal{N}, \mathcal{X}_k = \mathcal{C}_k + \mathcal{N}_k, k \in [1, K] \\ H_1 : \mathcal{X} = \alpha \mathbf{S} + \mathcal{C} + \mathcal{N}, \mathcal{X}_k = \mathcal{C}_k + \mathcal{N}_k, k \in [1, K] \end{cases} \quad (54)$$

- Using Proposition 3.2, the data are preprocessed in order to remove the LR contribution. We denote $\mathbb{A}_1 \dots \mathbb{A}_L = \times_{\mathbb{A}_1} \mathbf{U}_0^{(\mathbb{A}_1)} \mathbf{U}_0^{(\mathbb{A}_1)H} \dots \times_{\mathbb{A}_L} \mathbf{U}_0^{(\mathbb{A}_L)} \mathbf{U}_0^{(\mathbb{A}_L)H}$. The hypothesis test becomes

$$\begin{cases} H_0 : \mathcal{X}_{\mathbb{A}_1 \dots \mathbb{A}_L} = \mathcal{N}_{\mathbb{A}_1 \dots \mathbb{A}_L}, \mathcal{X}_{k, \mathbb{A}_1 \dots \mathbb{A}_L} = \mathcal{N}_{k, \mathbb{A}_1 \dots \mathbb{A}_L} \\ H_1 : \mathcal{X}_{\mathbb{A}_1 \dots \mathbb{A}_L} = \alpha \mathbf{S}_{\mathbb{A}_1 \dots \mathbb{A}_L} + \mathcal{N}_{\mathbb{A}_1 \dots \mathbb{A}_L}, \\ \mathcal{X}_{k, \mathbb{A}_1 \dots \mathbb{A}_L} = \mathcal{N}_{k, \mathbb{A}_1 \dots \mathbb{A}_L} \end{cases} \quad (55)$$

- Then, the operator vec is applied, which leads to

$$\begin{cases} H_0 : \text{vec}(\mathcal{X}_{\mathbb{A}_1 \dots \mathbb{A}_L}) = \text{vec}(\mathcal{N}_{\mathbb{A}_1 \dots \mathbb{A}_L}), \\ \text{vec}(\mathcal{X}_{k, \mathbb{A}_1 \dots \mathbb{A}_L}) = \text{vec}(\mathcal{N}_{k, \mathbb{A}_1 \dots \mathbb{A}_L}) \\ H_1 : \text{vec}(\mathcal{X}_{\mathbb{A}_1 \dots \mathbb{A}_L}) = \alpha \text{vec}(\mathbf{S}_{\mathbb{A}_1 \dots \mathbb{A}_L}) + \text{vec}(\mathcal{N}_{\mathbb{A}_1 \dots \mathbb{A}_L}), \\ \text{vec}(\mathcal{X}_{k, \mathbb{A}_1 \dots \mathbb{A}_L}) = \text{vec}(\mathcal{N}_{k, \mathbb{A}_1 \dots \mathbb{A}_L}) \end{cases} \quad (56)$$

where

$$\text{vec}(\mathcal{N}_{\mathbb{A}_1 \dots \mathbb{A}_L}), \text{vec}(\mathcal{N}_{k, \mathbb{A}_1 \dots \mathbb{A}_L}) \sim \mathcal{CN}(\mathbf{0}, \sigma^2 \mathbf{I}_{I_1 \dots I_p}).$$

- The problem is then to detect a signal $\text{vec}(\mathbf{S}_{\mathbb{A}_1 \dots \mathbb{A}_L})$ corrupted by a white noise $\text{vec}(\mathcal{N}_{\mathbb{A}_1 \dots \mathbb{A}_L})$. Since α and σ are unknown, the adaptive normalized matched filter introduced in [30] can be applied:

$$\begin{aligned}
 \Lambda_{\mathbb{A}_1 \dots \mathbb{A}_L} &= \frac{|\langle \text{vec}(\mathbf{S}_{\mathbb{A}_1 \dots \mathbb{A}_L}), \text{vec}(\mathcal{X}_{\mathbb{A}_1 \dots \mathbb{A}_L}) \rangle|^2}{\langle \text{vec}(\mathbf{S}_{\mathbb{A}_1 \dots \mathbb{A}_L}), \text{vec}(\mathbf{S}_{\mathbb{A}_1 \dots \mathbb{A}_L}) \rangle \langle \text{vec}(\mathcal{X}_{\mathbb{A}_1 \dots \mathbb{A}_L}), \text{vec}(\mathcal{X}_{\mathbb{A}_1 \dots \mathbb{A}_L}) \rangle} \quad (57)
 \end{aligned}$$

- Finally, the proposition is proven by applying the operator vec^{-1} .

Competing interests

The authors declare that they have no competing interests.

Author details

¹SATIE, ENS Cachan, 61, av President Wilson, Cachan 94230, France. ²SONDRA, Supélec, 3 rue Joliot-Curie, Gif-sur-Yvette 91192, France. ³LISTIC - Polytech Annecy-Chambéry, 5, chemin de Bellevue, Annecy le Vieux 74944, France.

Received: 4 April 2014 Accepted: 14 July 2014

Published: 30 July 2014

References

- M Boizard, G Ginolhac, F Pascal, P Forster, A new tool for multidimensional low-rank STAP filter: cross HOSVDs, in *Proceedings of EUSIPCO* (Bucharest, Romania, September 2012)
- T Kolda, B Bader, Tensor decompositions and applications. *SIAM Rev.* **51**, 455–500 (2009)
- LD Lathauwer, BD Moor, J Vandewalle, A multilinear singular value decomposition. *SIAM J. Matrix Anal. Appl.* **24**(4), 1253–1278 (2000)
- RA Harshman, Foundation of the PARAFAC procedure: model and conditions for an explanatory multi-mode factor analysis. *UCLA Working Pap. Phon.* **16**, 1–84 (1970)
- ND Sidiropoulos, R Bro, GB Giannakis, Parallel factor analysis in sensor array processing. *IEEE Trans. Proc. Sig. Proc.* **48**(8), 2377–2388 (2000)
- ND Sidiropoulos, R Bro, GB Giannakis, Blind PARAFAC receivers for DS-CDMA systems. *IEEE Trans. Proc. Sig. Proc.* **48**(3), 810–823 (2000)
- ALF de Almeida, G Favier, JCM Mota, Constrained Tucker-3 model for blind beamforming. *Elsevier Signal Process.* **89**, 1240–1244 (2009)
- G Favier, MN da Costa, ALF de Almeida, JMT Romano, Tensor space time (TST) coding for MIMO wireless communication systems. *Elsevier Signal Process.* **92**, 1079–1092 (2012)
- LR Tucker, Some mathematical notes on three-mode factor analysis. *Psychometrika.* **31**, 279–311 (1966)
- I Kirsteins, D Tufts, Adaptive detection using a low rank approximation to a data matrix. *IEEE Trans. Aero. Elec. Syst.* **30**, 55–67 (1994)
- A Haimovich, Asymptotic distribution of the conditional signal-to-noise ratio in an eigenanalysis-based adaptive array. *IEEE Trans. Aero. Elec. Syst.* **33**, 988–997 (1997)
- P Comon, Tensors : a brief introduction. *IEEE Signal Process. Mag.* **31**(3), 44–53 (2014)
- LD Lathauwer, Decompositions of a higher-order tensor in block terms-part I: lemmas for partitioned matrices. *SIAM J. Matrix Anal. Appl.* **30**(3), 1022–1032 (2008)
- D Muti, S Bourennane, Multidimensional filtering based on a tensor approach. *Elsevier Signal Process.* **85**, 2338–2353 (2005)
- NL Bihan, G Ginolhac, Three-mode data set analysis using higher order subspace method: application to sonar and seismo-acoustic signal processing. *Elsevier Signal Process.* **84**(5), 919–942 (2004)
- M Haardt, F Roemer, GD Galdo, Higher-order SVD-based subspace estimation to improve the parameter estimation accuracy in multidimensional harmonic retrieval problems. *IEEE Trans. Proc. Sig. Proc.* **56**(7), 3198–3213 (2008)
- LD Lathauwer, BD Moor, J Vandewalle, Independent component analysis and (simultaneous) third-order tensor diagonalization. *IEEE Trans. Sig. Proc.* **49**, 2262–2271 (2001)
- MAO Vasilescu, D Terzopoulos, Multilinear subspace analysis of image ensembles, in *Proc. of the IEEE Conf. on Computer Vision and Pattern Recognition*, (June 2003)
- J Salmi, A Richter, V Koivunen, Sequential unfolding SVD for tensors with applications in array signal processing. *IEEE Trans. Sig. Proc.* **57**(12), 4719–4733 (2009)
- J Ward, Space-time adaptive processing for airborne radar. Technical report. Lincoln Lab., MIT, Lexington, Mass., USA (December 1994)
- LE Brennan, FM Staudaher, Subclutter visibility demonstration. Technical report. RL-TR-92-21, Adaptive Sensors Incorporated (March 1992)
- G Showman, W Melvin, M Belenkii, Performance evaluation of two polarimetric STAP architectures, in *Proc. of the IEEE Int. Radar Conf.*, (May 2003), p. 59–65
- VF Mecca, D Ramakrishnan, JL Krolik, MIMO radar space-time adaptive processing for multipath clutter mitigation, in *Fourth IEEE Workshop On Sensor Array and Multichannel Processing*, 2006, (July 2006), p. 249–253
- CY Chen, PP Vaidyanathan, A subspace method for MIMO radar space-time adaptive processing, in *IEEE International Conference on ICASSP 2007* (Honolulu, Hawaii, USA, 2007), p. 925–928
- CY Chen, PP Vaidyanathan, MIMO radar space-time adaptive processing using prolate spheroidal wave functions. *IEEE Trans. Sig. Proc.* **56**(2), 623–635 (2008)
- R Fa, RC de Lamare, P Clarke, Reduced-rank STAP for MIMO radar based on joint iterative optimization of knowledge-aided adaptive filters, in *2009 Conference Record of the Forty-Third Asilomar Conference On Signals, Systems and Computers*, pp. 496–500
- LD Lathauwer, BD Moor, J Vandewalle, On the best rank-1 and rank- (r_1, r_2, \dots, r_n) approximation and applications of higher-order tensors. *SIAM J. Matrix Anal. Appl.* **21**(4), 1324–1342 (2000)
- S Miron, NL Bihan, J Mars, Vector-sensor MUSIC for polarized seismic sources localization. *EURASIP J. Adv. Signal Process.* **2005**, 74–84 (2005)
- IS Reed, JD Mallett, LE Brennan, Rapid convergence rate in adaptive arrays. *IEEE Trans. Aero. Elec. Syst.* **AES-10**(6), 853–863 (1974)
- LL Scharf, B Friedlander, Matched subspace detector. *IEEE Trans. Sig. Proc.* **42**(8), 2146–2157 (1994)
- M Rangaswamy, FC Lin, KR Gerlach, Robust adaptive signal processing methods for heterogeneous radar clutter scenarios. *Elsevier Signal Process.* **84**, 2004
- LD Lathauwer, Decompositions of a higher-order tensor in block terms-part II definitions and uniqueness. *SIAM J. Matrix Anal. Appl.* **30**(3), 1033–1066 (2008)
- LD Lathauwer, D Nion, Decompositions of a higher-order tensor in block terms - part III: alternating least squares algorithms. *SIAM J. Matrix Anal. Appl.* **30**(3), 1067–1083 (2008)
- G Ginolhac, P Forster, F Pascal, JP Ovarlez, Performance of two low-rank STAP filters in a heterogeneous noise. *IEEE Trans. Signal Process.* **61**, 57–61 (2013)
- LE Brennan, LS Reed, Theory of adaptive radar. *IEEE Trans. Aero. Elec. Syst.* **9**(2), 237–252 (1973)

doi:10.1186/1687-6180-2014-119

Cite this article as: Boizard et al.: Low-rank filter and detector for multidimensional data based on an alternative unfolding HOSVD: application to polarimetric STAP. *EURASIP Journal on Advances in Signal Processing* 2014 **2014**:119.

Submit your manuscript to a SpringerOpen[®] journal and benefit from:

- Convenient online submission
- Rigorous peer review
- Immediate publication on acceptance
- Open access: articles freely available online
- High visibility within the field
- Retaining the copyright to your article

Submit your next manuscript at ► springeropen.com